Available online at www.sciencedirect.com

ScienceDirect

Advances in Space Research 71 (2023) 5493–5501

ADVANCES IN SPACE RESEARCH (a COSPAR publication)

www.elsevier.com/locate/asr

Seyfert-1 galaxies in WINGS and Omega-WINGS ☆

Paola Marziani [a,*], Mauro D'Onofrio [b,1], Mario Radovich [a], Alessia Moretti [a], Bianca M. Poggianti [a]

[a] National Institute for Astrophysics (INAF), Padua Astronomical Observatory, Vicolo dell' Osservatorio 5, Padua IT35122, Italy
[b] University of Padua, Department of Physics & Astronomy, Vicolo dell' Osservatorio 3, Padua IT35122, Italy

Received 30 October 2022; received in revised form 2 February 2023; accepted 14 February 2023
Available online 21 February 2023

Abstract

Type-1 nuclear activity is rare in low-redshift clusters of galaxies. An analysis of the WIde field Nearby Galaxy Cluster Survey (WINGS) and of its extension Omega-WINGS revealed only three Seyfert 1 galaxies that are cluster members. We present a focused analysis of their emission line properties according to the interpretation scheme known as the Eigenvector 1/main sequence of quasars. Nuclear activity of the cluster members appears to be modest in the context of low-z type-1 AGN; however, one of the three Seyfert galaxies (WINGS J201158.35–570512.1) is a candidate super-Eddington source. Some general implications on non-thermal activity in clusters are suggested by the low prevalence of Seyfert 1s in the survey, and by the prevalence ratio between type-2 and type-1 AGN, apparently much higher in the cluster environment than in the field.

Keywords: Active galactic nuclei; Clusters of galaxies; Quasar main sequence

1. Introduction

Nuclear activity has been thought to be rare in cluster of galaxies since the earliest works in the 1970s (Dressler et al., 1985). Later surveys confirmed the early results as far as low-redshift clusters are concerned (von der Linden et al., 2010; Hwang et al., 2012; Pimbblet et al., 2013). For instance, a lower AGN fraction in clusters than for the fields in large samples of X-ray selected clusters has been detected from the ROSAT below $z \lesssim 0.5$ (Mishra and Dai, 2020). AGN properties are consistent with a relatively gas-poor environment, with a large fraction of cluster galaxies showing signs of very low-level activity (e.g., Balick and Heckman, 1982; Marziani et al., 2017). There is however an intriguing dichotomy between optical and X-ray detections: X ray data indicate frequent AGN detection in the outer regions of clusters (Koulouridis et al., 2018; Koulouridis and Bartalucci, 2019), but the relation between optically detected activity (i.e., via diagnostic diagrams) and X-ray detections (Martini et al., 2002; Martini et al., 2006) remains unclear to-date.

A relevant question is how cluster properties affect the frequency of AGN, especially at high redshift. Recent studies are now tackling redshifts as high as 1 and unanimously detect positive evolution in the sense that there is an increasing fraction of AGN with increasing redshift in clusters (e.g., Martini et al., 2009; Martini et al., 2013; Bufanda et al., 2017; Krishnan et al., 2017) and in the general population of galaxies as well (e.g., Hopkins et al., 2006; Shankar et al., 2013). Large amount of gas and high rate of galaxy interactions in high-redshift protoclusters are conductive to star formation and to the occurence of lumi-

☆ Oral contribution presented at the COSPAR XXIV General Assembly held in Athens on July 16-24, 2022, as part of Event E1.7 "Properties and Evolution of Active Galactic Nuclei in Galaxy Clusters".

* Corresponding author.
E-mail address: paola.marziani@inaf.it (P. Marziani).

[1] INAF associate.

https://doi.org/10.1016/j.asr.2023.02.029
0273-1177/

nous AGN. Not only, high radio activity among the massive galaxy population in clusters is found at redshift $z \sim 1$ (Mo et al., 2020). Low-mass or merging clusters show higher prevalence of AGN than fully virialized ones (Koulouridis et al., 2018).

This study focuses on the prevalence of type-1 AGN in clusters, and on the properties of the specimens that were identified. Unlike other AGN types, type-1 AGN are difficult to miss and misclassify even at a perfunctory visual inspection. Type-1 AGN also offer an unimpeded view of the central regions of the AGN allowing at least a coarse estimate of accretion parameters from optical survey data, and the exploitation of the so-called Eigenvector 1 - main sequence (E1/MS) correlations (Boroson and Green, 1992; Sulentic et al., 2000b; Shen and Ho, 2014). The backside is that type-1 AGN are expected to be extremely rare because any luminous AGN depletion in clusters is compounded with a low prevalence in the field. The sample is therefore drawn from one of largest surveys covering clusters at low redshift, the WIde field Nearby Galaxy Cluster Survey (WINGS; Section 2). The analysis of the spectra (Section 3) identifies a few candidates that are analyzed in detail following the E1/MS prescriptions (Section 4). Inferences from the cluster properties and from the prevalence of type-2 AGN (Section 5) suggest a possible scenario that remains however largely hypothetical due to the small number of involved sources.

2. WINGS spectroscopy

The core of the original WINGS project is an optical (B, V) imaging survey that provided photometric data for huge samples of galaxies (≈550,000) selected from X-ray bright clusters (Fasano et al., 2006). The selection criteria of the survey were as follows:

- X-ray (from ROSAT-RASS) flux above $f_X \approx (5.0, 4.4, 2.8) \cdot 10^{-12}$ erg cm^{-2} s^{-1} (Ebeling et al., 2000);
- Galactic latitude $|b| > 20$ deg;
- Redshift range $0.04 < z < 0.07$.

The spectroscopic counterpart of the photometric survey encompasses 48 clusters, observed with similar instrumental setups, yielding spectral resolving power $\lambda/\delta\lambda \sim 1000$. A summary of the spectroscopic properties is provided in Table 1 where number of galaxies observed in the survey, number of galaxies that are cluster member, fibre aperture, spectroscopic completeness and references are reported. The OmegaWINGS survey is an extension of the WINGS survey intended to extend out to large clustercentric distances ($1 - 5\, r_{200}$), probing the cluster outskirts and surrounding groups and filaments of 33 WINGS clusters (Moretti et al., 2017).

3. Analysis

The analysis i.e., the inspection of the rest-frame spectra to identify Seyfert 1 nuclei was carried out on the stacked cluster sample of all 48 clusters that includes more than 11,000 cluster member galaxies. In other words, estimates of prevalences were made as if the cluster member galaxies were belonging to a unique cluster built as the union of the individual clusters.

The optical spectra of the singled-out Seyfert 1 candidates were modelled as the sum of several components according to the prescription of the E1/MS correlations (Section 4). The continuum was modelled as the sum of a power law component and an evolved ($t > 5$ Gyr) and less-evolved stellar populations (Bruzual and Charlot, 2003), allowing internal extinction (values found were around $A_V \approx 0.2$ mag). The broad emission features included in the model were HI broad Balmer lines Hβ and Hα, a scaled and broadened FeII template, and narrow lines. The [OIII]$\lambda\lambda$4959,5007 was modelled as the sum of narrow and blueshifted semibroad component (Marziani et al., 2022, and references therein). A best fit was sought applying χ^2_ν minimization techniques within the IRAF task `specfit` (Kriss, 1994).

4. Results

The visual inspection of all 11,128 galaxy spectra identified 3 Seyfert 1 galaxies: 2 Pop. B (WINGS J043838.78–220325.0 in Abell 500 and WINGS J060131.87–401646.9 in Abell 3376), and 1 extreme Pop. A following Sulentic et al. (2000a): WINGS J201158.35–570512.1 in Abell 3667, as well as 5 Seyfert 1.9 (presumably all of Population B). Spectra are shown in Fig. 1–3.

Population B sources are low accretors with $L/L_{\rm Edd} \lesssim 0.2$, "disk dominated" i.e., without the prominent winds observable in the UV and optical spectra of Population A (Sulentic et al., 2000b; Shen and Ho, 2014). On the converse, Population A refers to sources with FWHM(Hβ) $\lesssim$ 4000 km s^{-1}, Population B to sources with Hβ broader than this limit. Population A sources are moderate/high accretors that radiate at an Eddington ratio $L/L_{\rm Edd}$

Table 1
Properties of the stacked WINGS spectroscopic sample of 48 clusters.

Survey	N		AGN		Fiber size	Completeness	Refs.
	galaxies	cluster members	type-1	type-2			
WINGS-SPE	6137	3647	2	34	1.6"/2.0"	50% down to V = 19	Cava et al., 2009
OmegaWINGS	17985	7479	1	...	2.16"	80% down to V = 20	Moretti et al., 2017

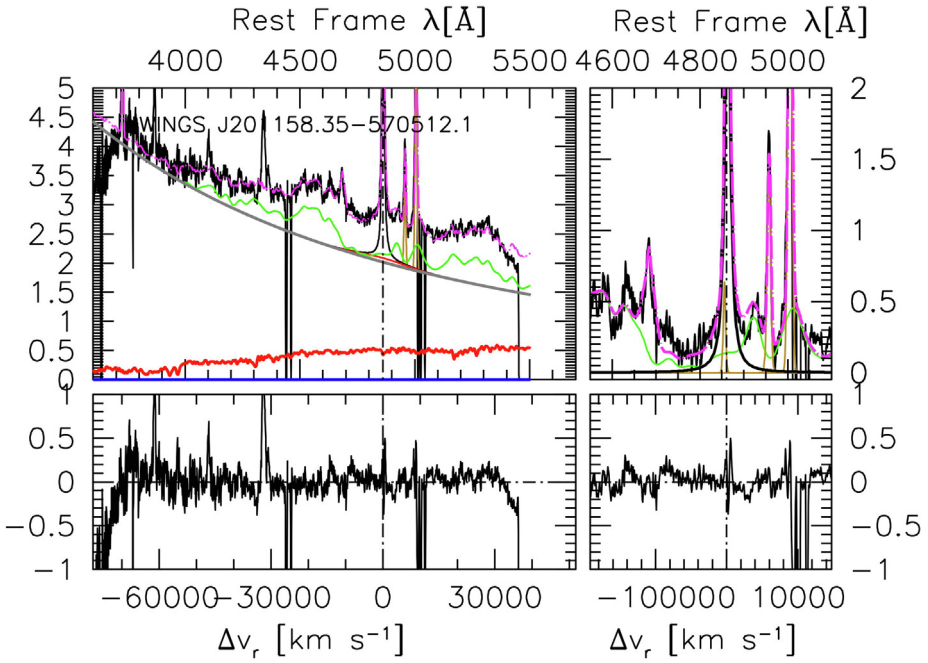

Fig. 1. Spectrum of WINGS J201158.35–570512.1 in Abell 3667, the sole highly accreting source identified in the more than 11,000 galaxies of WINGS + OMEGAWINGS. The left panels show the spectral range ≈ 3700 − 5500 that includes [OII]λ3727 at its blue end and the FeII optical blends at blue and red side of Hβ. The upper panel shows the original spectrum in the rest frame (black line), the assumed power-law continuum (grey), the FeII emission template (lemon green), the $H\beta_{BC}$ (thick black), the [OIII]λλ4959,5007 and [OII]λ3727 narrow line (gold) and the continuum of an evolved stellar population representing the host galaxy. The vertical scale is flux normalized at 5100 Å. The bottom panel shows the residual observed spectrum minus model. Right panel: same, after continuum subtraction, in a narrower wavelength range to better show the profiles of Hβ and [OIII]λλ4959,5007. The sharp absorptions around 4400 Å and 5100 Å are instrumental defects.

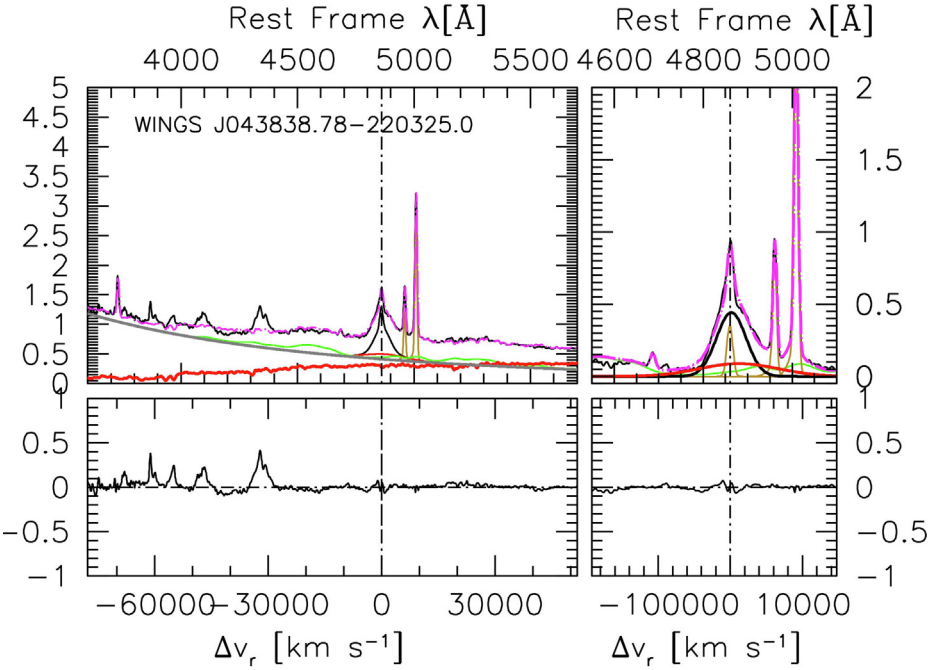

Fig. 2. Spectrum of a Population B source. Meaning of the color code is the same as for Fig. 1. In this case however, the Hβ broad profile has been decomposed into a $H\beta_{BC}$ (thick black line) and a very broad component $H\beta_{VBC}$ (thick red line). The decomposition provides a very good fit to the Hβ broad profile, as found for the wide majority of Population B sources in luminous type-1 AGN samples.

$\gtrsim 0.2$, "wind dominated' (Richards et al., 2011), and that include a population of extreme (xA) sources radiating at $L/L_{Edd} \gtrsim 1$. The different L/L_{Edd} along with several phenomenological differences (reviewed by Marziani et al., 2018) suggest different accretion structures in Population A and B, with Population B associated with a geometrically

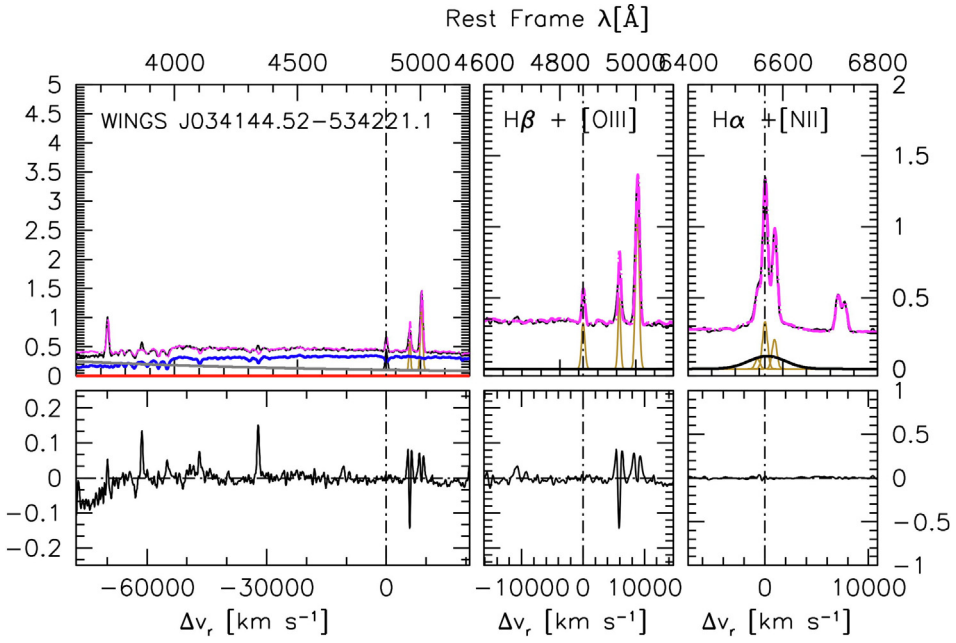

Fig. 3. Spectrum of WINGS J034144.52–534221.1, a type-1.9 Seyfert, with no detectable emission in FeIIλ4570. Meaning of the color code is the same as for Fig. 1. A third panel has been added to show the spectral range around Hα.

thin, optically thick accretion disk around a supermassive black hole. Population A is expected to have an inner radiation-pressure supported, optically and geometrically thick accretion disk (Abramowicz et al., 1988). Extreme Population A may accrete at highly super-Eddington rates (Wang et al., 2013; Giustini and Proga, 2019).

Fig. 4 showing the optical plane defined by FWHM(Hβ) and prominence of singly-ionized iron emission is the projection of multi-frequency "Eigenvector 1" correlation space, and is mainly a sequence of Eddington ratio convolved with the effect of viewing angle and black hole mass (Marziani et al., 2001; Boroson, 2002; Shen and Ho, 2014; Panda et al., 2019). The presence of an extreme Population A object is outstanding, since the prevalence of Pop. A and B is roughly the same in the field. WINGS J201158.35–570512.1 ($\equiv$ Fairall 339, Fairall, 1981) is the sole Population A AGN and all others are presumably Population B consistent with modest level of activity. Note that the elliptical shaded area indicating the loci of type-1.9 sources is purely indicative, and based on the width of the Hα broad line, and on the absence of any detectable FeII emission in the spectral range of Hβ, and not on an actual $R_{\rm FeII}$ measurement. Attempts were made to detect broad Hβ and FeII emission but they are lost in the spectrum of the host galaxy. The distribution of Eddington ratios for the S1.9 sources peaks at $L/L_{\rm Edd} \sim 10^{-2}$, a value consistent with their classification as Population B sources (Fig. 5). Luminosities were estimated from the absolute magnitude scaled to the AGN continuum fraction. A standard bolometric correction equal to 10 has been applied to the luminosity at 5100 Å (e.g., Richards et al., 2006). The black hole mass $M_{\rm BH}$ has been computed from the luminosity at 5100 Å and the FWHM of Hβ or Hα as they should be interchangeable in the same object (Rakić, 2022) applying the standard scaling law of Vestergaard and Peterson (2006). Masses and Eddington ratios are typical of low-redshift type-1 AGN. At low luminosity, all Pop. B sources with good data show $R_{\rm FeII} \lesssim 0.5$: this motivates the shaded area even without individual $R_{\rm FeII}$ measurements.

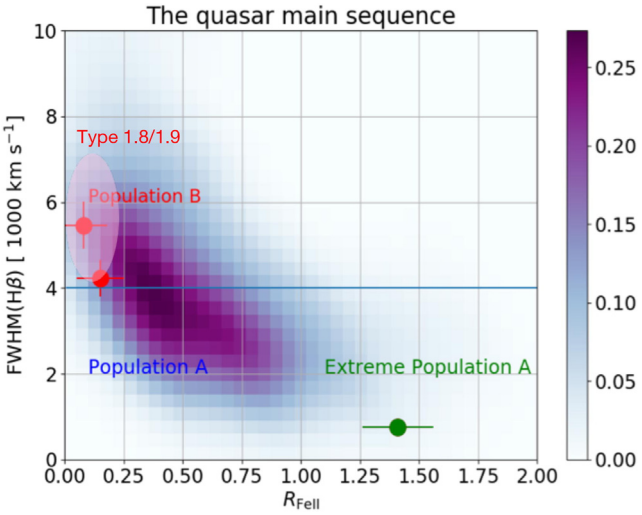

Fig. 4. Optical plane of the E1 MS defined by the FeII prominence parameter $R_{\rm FeII}$ and by the FWHM of broad Hβ. The three circles mark the location of the Seyfert 1 nuclei (2 Population B and 1 Population A). The shaded areas are color-coded according to the occupation of the plane in a large SDSS-based sample of type-1 Seyfert 1 and low-redshift quasars (Zamfir et al., 2010). The semi-transparent ellipse identifies the putative loci of the Type 1.9 AGN detected in the survey. The line at 4000 km s^{-1} marks the boundary between Population A and B.

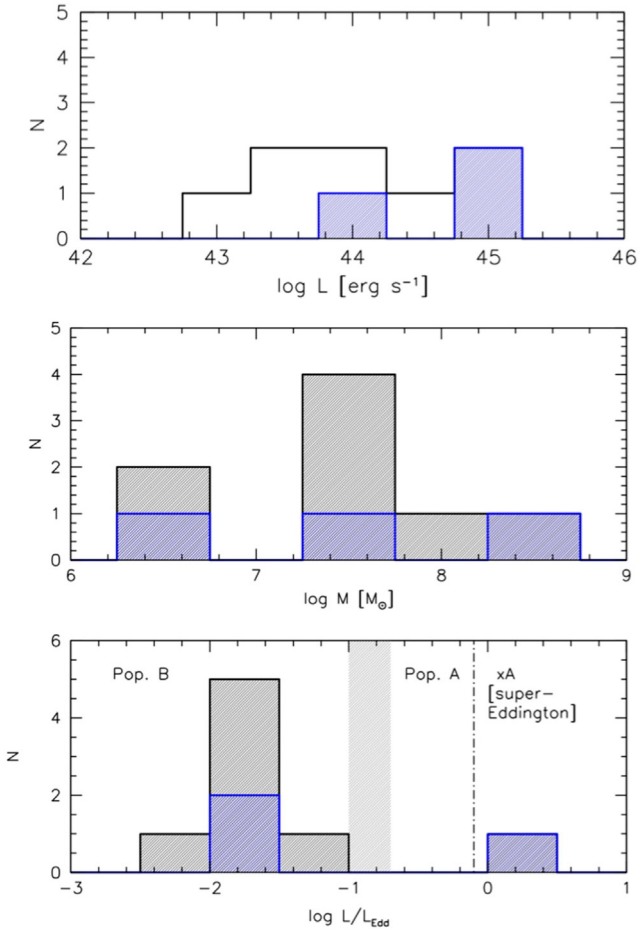

Fig. 5. Luminosity, black hole mass $M_{\rm BH}$ and Eddington ratio $L_{\rm Edd}$ - distributions for the Seyfert 1 and intermediate Seyfert 1 in WINGS. The low Eddington ratio for the intermediate systems is consistent with their classification as Population B. Sources. The grey strip delimits the $L/L_{\rm Edd}$ boundary between Pop. A and B, $\log L/L_{\rm Edd} \approx 0.1 - 0.2$.

Population B sources are almost 90% of the detected type-1.x AGN in WINGS, but perhaps the most striking result is, as mentioned, the detection of an extreme accretor in the cluster environment, at about 0.5 r_{200} cluster-centric distance, and with redshift $z \approx 0.0547 \pm 0.00042$ (Moretti et al., 2017) consistent with the redshift of its parent cluster, Abell 3667. Such sources are extreme in many aspects: Eddington ratio (Du et al., 2016a), accretion rate (Mineshige et al., 2000; Sdowski et al., 2014), outflow power (Leighly, 2004) and metal content (Śniegowska et al., 2021; Garnica et al., 2022). If $R_{\rm FeII} \gtrsim 1.5$ they account for ≈ 3% of color selected samples. Their importance is due – apart from the intrinsic interest for super-Eddington accretion – to the fact that they have been proposed as cosmological distance indicators (Wang et al., 2013; Dultzin et al., 2020). The main MS parameters of WINGS J201158.35–570512.1 ($R_{\rm FeII} \approx 1.4$, FWHM H$\beta \approx$ 760 km s^{-1}, $L/L_{\rm Edd} \approx 1.4$) are consistent with the local Narrow Line Seyfert 1 (NLSy1, or extreme Population A following Sulentic et al., 2000a) I Zw1, a prototypical xA: $R_{\rm FeII} \approx 1.6$, FWHM H$\beta \approx$ 1100 km s^{-1}, $L/L_{\rm Edd} \approx$ 1.45. The X-ray and infrared properties are also consistent with a highly accreting source: the ROSAT soft-X photon index is $\Gamma_{\rm soft} \approx 3.14$ (Boller et al., 2016), and the X ray 2 – 10 keV photon index measured on an XMM spectrum obtained on Oct. 2, 2000 is ≈ 3.32 (c.f. Laurenti et al., 2022). WINGS J201158.35–570512.1 appears a peculiar source in cluster environment: blue color index ($B - V \approx 0.50$, Souchay et al., 2015), late-type spiral morphology Sd (possibly perturbed) and IRAS detection associated with a FIR luminosity $L_{60\mu m} \approx 1.3 \cdot 10^{44}$ erg s^{-1} corresponding to a SFR ∼ 12.4 M$_\odot$ yr^{-1} (Li et al., 2010). WINGS J201158.35–570512.1 is found in a cluster (Abell 3667) that is the result of a merging process between two main sub-clusters (Owers et al., 2009). Its location in the plane defined by the projected linear distance r/r_{200} and by redshift difference δz between the source and the brightest cluster galaxy normalized by the cluster dispersion $\sigma_{\rm cl}$ (Fig. 6) supports actual cluster membership. The Population B Seyfert 1 and Seyfert 1.x host galaxies are morphologically early-type spirals (the latest time is Sa), with stellar masses in the range $\log M_\star \sim 10.5 - 10.5[M_\odot]$ (Fritz et al., 2011).

5. Discussion

5.1. A hint to cluster properties that are AGN–hosting

Are the clusters that host AGN systematically different from the other clusters? The WINGS is made of low redshift, fairly evolved clusters. Nonetheless the majority of the WINGS cluster presents sub-structures indicative of multiple systems, possibly in collision and of absence of virialization (Ramella et al., 2007; Valentinuzzi et al.,

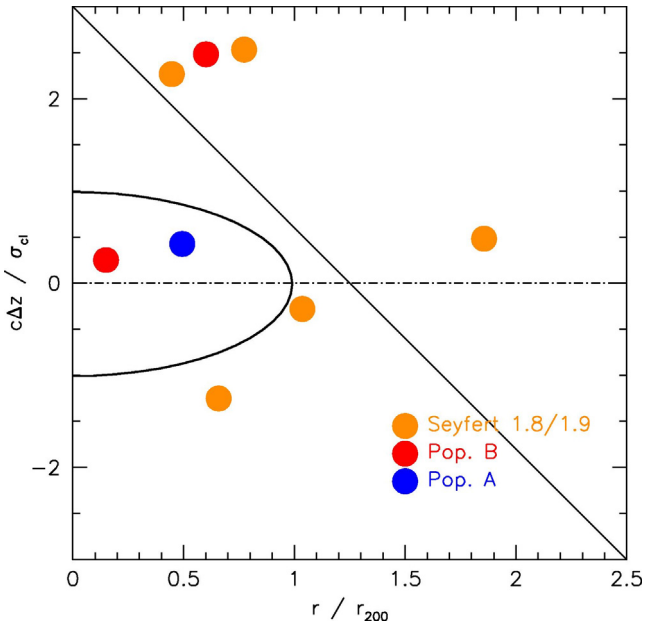

Fig. 6. Distribution of the AGN in the plane r/r_{200} and $\Delta z/\sigma_{\rm cl}$. The thick line marks the loci with $r/r_{200} = 1$ and $c\delta z/\sigma_{\rm cl} = 1$.

2011). The number of clusters is very small so that the following result will need confirmation from larger samples. However, if we consider the number of substructures N_{sub} times the luminosity fraction of the cluster emitted in the substructures as listed by Valentinuzzi et al. (2011), we obtain $\left(N_{sub} \cdot \frac{L_{sub}}{L_{main}}\right)_{Seyf1} \approx 2\left(N_{sub} \cdot \frac{L_{sub}}{L_{main}}\right)_{noAGN}$ i.e., that the luminosity fraction confined to substructures is twice larger for clusters that host AGN with respect to those that do not. This result is consistent with other surveys and with the overall trends of increase of AGN prevalence with redshift: at $z \approx 1$ clusters were overall less virialized than at present cosmic epochs. Of 46 WINGS clusters only 18 have type-2 or type 1 AGN; and of the 18, 12 have more than 1 detected AGN. Of the 15 with available data, only 5 do not have substructures recognized by Ramella et al. (2007).

5.2. The prevalence of Seyfert 1s and the type-2 to type-1 ratio

The "old lore" of AGN states that the prevalence of Seyfert 1 galaxies is around $\approx 1\%$ of luminous galaxies (Osterbrock and Ferland, 2006), with a type-2 to type-1 ratio consistent with 2.0:1.0 (Antonucci, 1993). Surveys carried out in the 1990s and 2000s basically confirm the "old lore" scenario, finding prevalence $\sim 1\%$ for Seyfert 1, and type-2 to type-1 ratio between 2:0 and 3:0, for luminous galaxies with $M_B \lesssim -20$ (Huchra and Burg, 1992; Kinney et al., 2000; Maia et al., 2003). Here we utilize for comparison several not-so recent surveys that might be affected by similar selection effects as WINGS: only a coarse comparison between the WINGS results and the results of the previous surveys is possible without accounting for completeness effects; however, for the WINGS + OmegaWINGS sample, considering also intermediate Seyferts (all type 1.9 sources that would have been likely missed in large fraction in the previous surveys; at the same time, a caveat of the present sample is that Seyfert 1.9 might have been missed due to the difficulty to correct for the B-band telluric absorption that strongly affects the Hα range at $z \approx 0.05$) we obtain a prevalence ≈ 0.1 %, a factor 10 below previous results for field galaxies.

A comparison between the prevalence of type 1 and type 2 is possible only from the catalog of Marziani et al. (2017) for the WINGS sample. The catalog reports probabilities of classification for Seyfert, HII, LINERs and transition objects on the basis of four diagnostic diagrams: [OII]λ3727/Hβ, [OI]λ6300/Hα, [NII]λ6583/Hα, SII]λ6717,6730/Hα vs. [OIII]/Hβ (Baldwin et al., 1981; Veilleux and Osterbrock, 1987). The [OII]λ3727/Hβ and [NII]λ6583/Hα provide the most reliable diagnostics. There are 34 sources meeting the Seyfert classifications in the two diagnostic diagrams against 2 Seyfert 1 (Pop. B) and 1 intermediate Seyfert, suggesting a type-2 to type-1 ratio ~ 10. The ratio of the frequency of type-2 and type-1 AGN appears to be much higher than in the field (see also Mo et al. (2018) who found a large excess of type-2 AGN in the central arcminute of clusters at redshift ≈ 1), which may hint toward some form of widespread, obscured (Compton-thick?) low-level activity. This estimate is conservative: if only the [NII]λ6583/Hα diagram were considered, the ratio would be above 20.

5.2.1. Implications for Unification Schemes?

What kind of type-1 AGN are (obscured) type-2 AGN? This question is as yet unanswered. Obscured type 2 such as NGC 1068 are sources accreting at a high rate from the R_{FeII} ratio measured in polarized light (Antonucci and Miller, 1985; Du et al., 2016b). However, at the low end of AGN activity, sources might show extremely broad and vanishingly weak broad lines (Laor, 2003). The maximum observed full width zero intensity (FWZI) is $\approx 30,000$ km s^{-1} for Population B objects, with FWZI $\approx 2v_{in} \sin\theta$, where v_{in} is the innermost velocity within the BLR, and θ is the angle between the accretion disk axis (assumed as the plane of symmetry of the BLR) and the line-of-sight. In the case of a flattened emitting region with a virial velocity field this would correspond to a distance from the central black hole $r_{in} \approx (4c^2 \sin^2\theta/\mathrm{FWZI}^2) r_g$ gravitational radii (c.f. Punsly et al., 2020), $r_{in} \sim 100 r_g$, if $\theta \approx 30$ degrees. Below 100 r_g optical lines might not be prominently emitted, as the disk is too hot and the accretion flow might be advection-dominated (Giustini and Proga, 2019). For a virial velocity field and a scaling law $r \propto L^a$ (Bentz et al., 2013), the velocity dispersion is scaling as ${L/L_{Edd}}^{-a/2}$. A limiting width corresponds to the lower boundary in L/L_{Edd}, beyond which no broad line emission is possible. Such sources – radiating at very low Eddington ratio $\lesssim 10^{-3}$ – would emit a narrow line spectrum consistent with the one of type 2 due to the prominent X-ray emission expected in the accretion regime of an advection-dominated ion torus (e.g.,Giustini and Proga, 2019, and references therein). In this view, the presence of low-level, type-2 activity could just reflect the scarcity of atomic gas in the interstellar medium of cluster galaxies, most likely driven by gas supply starvation and ram-pressure stripping of cold gas (D'Onofrio et al., 2015; Brown et al., 2017; Marziani et al., 2017).

5.2.2. The brightest cluster galaxies of WINGS

The paucity/weakness scenario of nuclear activity is not challenged by the presence of nuclear activity in brightest cluster galaxies. Of the 44 clusters of WINGS studied by D'Onofrio et al. (2019), BCGs were spectroscopically observed only for 23 clusters of galaxies, as the survey was not intended to specifically address BCGs. Of these 23, only WINGS J010851.12–152423.0 (BCG of A151) is classified as a LINER/transition object. Of the remaining clusters, a search for spectra in literature identified 4 LINERs, and a strong radio-loud source, making up about 25% of the BCGs not covered by the survey. The majority appear line-less. For the remaining quarter no data are available. Since a type-1 AGN would most probably have

been noted, we tentatively conclude that there is no evidence of luminous type-1 nuclei in the BCGs of the survey in agreement with Somboonpanyakul et al. (2022) who found a very low prevalence ($\sim 1\%$) of active BCGs at low redshift.

6. Conclusion

The main sequence is a powerful tool to contextualize type-1 AGN properties also at low luminosity and in the cluster environment. A striking result is the near absence of nuclear activity due to rarity of AGN and modest level of activity. Unlike fibre spectra, integral field spectroscopic observations might be able to detect very low-level activity at greater efficiency. The GASP survey based on MUSE (Poggianti et al., 2017; Radovich et al., 2019) indeed detects an excess in galaxies that are ram pressure stripped (Peluso et al., 2022). Seyfert 1s may preferentially occur in clusters with prominent sub-structures, but small number statistics makes this inference uncertain. The high Seyfert 2/Seyfert 1 number ratio appears perhaps as a more robust results. The implications for the strong unification scheme could be in the sense of a revision dependent on the galactic environment, as suggested (Dultzin-Hacyan et al., 1999; Krongold et al., 2003; Koulouridis, 2014).

In conclusion, there are some fundamental aspects of our understanding of the phenomenology of AGN in clusters, such as a dearth of activity in low-z cluster, with higher prevalence of AGN in the cluster outskirt, and an increase of the prevalence of AGN with increasing redshift that seems to be established. The issue remains however compounded with the still-debated extent of the effect that the environment may have on the nuclear activity of galaxies. Frontier aspects are now the definition of the apparently widespread X-ray detected activity, and the understanding of the complex interplay between the AGN feedback and the intra-cluster medium, as well as the environment provided by high-redshift clusters and proto-clusters that is apparently conductive to enhanced star formation and more widespread activity.

Declaration of Competing Interest

The authors declare that they have no known competing financial interests or personal relationships that could have appeared to influence the work reported in this paper.

References

Abramowicz, M.A., Czerny, B., Lasota, J.P., et al., 1988. Slim accretion disks. ApJ 332, 646–658. https://doi.org/10.1086/166683.

Antonucci, R., 1993. Unified models for active galactic nuclei and quasars. ARA&Ap 31, 473–521. https://doi.org/10.1146/annurev.aa.31.090193.002353.

Antonucci, R.R.J., Miller, J.S., 1985. Spectropolarimetry and the nature of NGC 1068. ApJ 297, 621–632. https://doi.org/10.1086/163559.

Baldwin, J.A., Phillips, M.M., Terlevich, R., 1981. Classification parameters for the emission-line spectra of extragalactic objects. PASP 93, 5–19. https://doi.org/10.1086/130766.

Balick, B., Heckman, T.M., 1982. Extranuclear clues to the origin and evolution of activity in galaxies. ARA&Ap 20, 431–468. https://doi.org/10.1146/annurev.aa.20.090182.002243.

Bentz, M.C., Denney, K.D., Grier, C.J., et al., 2013. The Low-luminosity End of the Radius-Luminosity Relationship for Active Galactic Nuclei. ApJ 767, 149. https://doi.org/10.1088/0004-637X/767/2/149, arXiv:1303.1742.

Boller, T., Freyberg, M.J., Trümper, J., et al., 2016. Second ROSAT all-sky survey (2RXS) source catalogue. A&Ap 588, A103. https://doi.org/10.1051/0004-6361/201525648, arXiv:1609.09244.

Boroson, T.A., 2002. Black hole mass and eddington ratio as drivers for the observable properties of radio-loud and radio-quiet QSOs. ApJ 565, 78–85. https://doi.org/10.1086/324486, arXiv:arXiv:astro-ph/0109317.

Boroson, T.A., Green, R.F., 1992. The emission-line properties of low-redshift quasi-stellar objects. Ap. J. Suppl. Ser. 80, 109. https://doi.org/10.1086/191661.

Brown, T., Catinella, B., Cortese, L., et al., 2017. Cold gas stripping in satellite galaxies: from pairs to clusters. Mon. Not. R. Astron. Soc. 466 (2), 1275–1289. https://doi.org/10.1093/mnras/stw2991, arXiv:https://academic.oup.com/mnras/article-pdf/466/2/1275/10866993/stw2991.pdf.

Bruzual, G., Charlot, S., 2003. Stellar population synthesis at the resolution of 2003. MNRAS 344, 1000–1028. https://doi.org/10.1046/j.1365-8711.2003.06897.x, arXiv:astro-ph/0309134.

Bufanda, E., Hollowood, D., Jeltema, T.E., et al., 2017. The evolution of active galactic nuclei in clusters of galaxies from the Dark Energy Survey. MNRAS 465 (3), 2531–2539. https://doi.org/10.1093/mnras/stw2824, arXiv:1606.06775.

Cava, A., Bettoni, D., Poggianti, B.M., et al., 2009. WINGS-SPE Spectroscopy in the WIde-field Nearby Galaxy-cluster Survey. A&Ap 495, 707–719. https://doi.org/10.1051/0004-6361:200810997, arXiv:0812.2022.

D'Onofrio, M., Marziani, P., Buson, L., 2015. The transformation of Spirals into S0 galaxies in the cluster environment. Front. Astron. Space Sci. 2, 4. https://doi.org/10.3389/fspas.2015.00004, arXiv:1508.04572.

D'Onofrio, M., Sciarratta, M., Cariddi, S., et al., 2019. The Parallelism between Galaxy Clusters and Early-type Galaxies. I. The Light and Mass Profiles. ApJ 875 (2), 103. https://doi.org/10.3847/1538-4357/ab1134, arXiv:1903.08692.

Dressler, A., Thompson, I.B., Shectman, S.A., 1985. Statistics of emission-line galaxies in rich clusters. ApJ 288, 481–486. https://doi.org/10.1086/162813.

Du, P., Lu, K.-X., Hu, C., et al., 2016a. Supermassive Black Holes with High Accretion Rates in Active Galactic Nuclei. VI. Velocity-resolved Reverberation Mapping of the Hβ Line. ApJ 820, 27. https://doi.org/10.3847/0004-637X/820/1/27, arXiv:1602.01922.

Du, P., Wang, J.-M., Hu, C., et al., 2016b. The fundamental plane of the broad-line region in active galactic nuclei. ApJL 818, L14. https://doi.org/10.3847/2041-8205/818/1/L14, arXiv:1601.01391.

Dultzin, D., Marziani, P., de Diego, J.A., et al., 2020. Extreme quasars as distance indicators in cosmology. Front. Astron. Space Sci. 6, 80. https://doi.org/10.3389/fspas.2019.00080, arXiv:2001.10368.

Dultzin-Hacyan, D., Krongold, Y., Fuentes-Guridi, I., et al., 1999. The close environment of seyfert galaxies and its implication for unification models. ApJ 513, L111–L114. https://doi.org/10.1086/311925, arXiv:arXiv:astro-ph/9901227.

Ebeling, H., Edge, A.C., Allen, S.W., et al., 2000. The ROSAT Brightest Cluster Sample - IV. The extended sample. MNRAS 318 (2), 333–340. https://doi.org/10.1046/j.1365-8711.2000.03549.x, arXiv:astro-ph/0003191.

Fairall, A.P., 1981. Spectroscopic survey of southern compact and bright-nucleus galaxies.IV. MNRAS 196, 417–424. https://doi.org/10.1093/mnras/196.3.417.

Fasano, G., Marmo, C., Varela, J., et al., 2006. WINGS: a WIde-field Nearby Galaxy-cluster Survey. I. Optical imaging. A&Ap 445, 805–817. https://doi.org/10.1051/0004-6361:20053816, arXiv:astro-ph/0507247.

Fritz, J., Poggianti, B.M., Cava, A., et al., 2011. WINGS-SPE II: A catalog of stellar ages and star formation histories, stellar masses and dust extinction values for local clusters galaxies. A&Ap 526, A45. https://doi.org/10.1051/0004-6361/201015214, arXiv:1010.2214.

Garnica, K., Negrete, C.A., Marziani, P., et al., 2022. High metal content of highly accreting quasars: Analysis of an extended sample. A&Ap 667, A105. https://doi.org/10.1051/0004-6361/202142837, arXiv:2208.02387.

Giustini, M., Proga, D., 2019. A global view of the inner accretion and ejection flow around super massive black holes. Radiation-driven accretion disk winds in a physical context. A&Ap 630, A94. https://doi.org/10.1051/0004-6361/201833810, arXiv:1904.07341.

Hopkins, P.F., Hernquist, L., Cox, T.J., et al., 2006. A Unified, Merger-driven Model of the Origin of Starbursts, Quasars, the Cosmic X-Ray Background, Supermassive Black Holes, and Galaxy Spheroids. Ap. J. Suppl. Ser. 163, 1–49. https://doi.org/10.1086/499298, arXiv:astro-ph/0506398.

Huchra, J., Burg, R., 1992. The spatial distribution of active galactic nuclei. I - The density of Seyfert galaxies and liners. ApJ 393, 90–97. https://doi.org/10.1086/171488.

Hwang, H.S., Park, C., Elbaz, D., et al., 2012. Activity in galactic nuclei of cluster and field galaxies in the local universe. A&Ap 538, A15. https://doi.org/10.1051/0004-6361/201117351, arXiv:1111.1973.

Kinney, A.L., Schmitt, H.R., Clarke, C.J., et al., 2000. Jet Directions in Seyfert Galaxies. ApJ 537 (1), 152–177. https://doi.org/10.1086/309016, arXiv:astro-ph/0002131.

Koulouridis, E., 2014. The dichotomy of Seyfert 2 galaxies: intrinsic differences and evolution. A&Ap 570, A72. https://doi.org/10.1051/0004-6361/201424622, arXiv:1408.6233.

Koulouridis, E., Bartalucci, I., 2019. High density of active galactic nuclei in the outskirts of distant galaxy clusters. A&Ap 623, L10. https://doi.org/10.1051/0004-6361/201935082, arXiv:1903.02919.

Koulouridis, E., Ricci, M., Giles, P., et al., 2018. The XXL Survey. XXXV. The role of cluster mass in AGN activity. A&Ap 620, A20. https://doi.org/10.1051/0004-6361/201832974, arXiv:1809.00683.

Krishnan, C., Hatch, N.A., Almaini, O., et al., 2017. Enhancement of AGN in a protocluster at z = 1.6. MNRAS 470 (2), 2170–2178. https://doi.org/10.1093/mnras/stx1315, arXiv:1705.10799.

Kriss, G., 1994. Fitting Models to UV and Optical Spectral Data. Astronomical Data Analysis Software and Systems III, A.S.P. Conf. Ser. 61, 437.

Krongold, Y., Dultzin-Hacyan, D., Marziani, P., 2003. An Evolutionary Sequence for AGN. In: Collin, S., Combes, F., Shlosman, I. (Eds.), Active Galactic Nuclei: From Central Engine to Host Galaxy. volume 290 of Astronomical Society of the Pacific Conference Series. p. 523.

Laor, A., 2003. On the Nature of Low-Luminosity Narrow-Line Active Galactic Nuclei. ApJ 590, 86–94. https://doi.org/10.1086/375008, arXiv:astro-ph/0302541.

Laurenti, M., Piconcelli, E., Zappacosta, L., et al., 2022. X-ray spectroscopic survey of highly accreting AGN. A&Ap 657, A57. https://doi.org/10.1051/0004-6361/202141829, arXiv:2110.06939.

Leighly, K.M., 2004. Hubble Space Telescope STIS Ultraviolet Spectral Evidence of Outflow in Extreme Narrow-Line Seyfert 1 Galaxies. II. Modeling and Interpretation. ApJ 611, 125–152. https://doi.org/10.1086/422089, arXiv:arXiv:astro-ph/0402452.

Li, Y., Calzetti, D., Kennicutt, R.C., et al., 2010. Spitzer 70 μ m emission as a star formation rate indicator for sub-galactic regions. ApJ 725, 677–691. https://doi.org/10.1088/0004-637X/725/1/677, arXiv:1010.0373.

Maia, M.A.G., Machado, R.S., Willmer, C.N.A., 2003. The seyfert population in the local universe. AJ 126 (4), 1750–1762. https://doi.org/10.1086/378360, arXiv:astro-ph/0307180.

Martini, P., Kelson, D.D., Kim, E., et al., 2006. Spectroscopic confirmation of a large population of active galactic nuclei in clusters of galaxies. ApJ 644, 116–132. https://doi.org/10.1086/503521, arXiv:astro-ph/0602496.

Martini, P., Kelson, D.D., Mulchaey, J.S., et al., 2002. An unexpectedly high fraction of active galactic nuclei in red cluster galaxies. ApJL 576, L109–L112. https://doi.org/10.1086/343729, arXiv:astro-ph/0208017.

Martini, P., Miller, E.D., Brodwin, M., et al., 2013. The cluster and field galaxy active galactic nucleus fraction at z = 1–1.5: evidence for a reversal of the local anticorrelation between environment and AGN fraction. ApJ 768 (1), 1. https://doi.org/10.1088/0004-637X/768/1/1, arXiv:1302.6253.

Martini, P., Sivakoff, G.R., Mulchaey, J.S., 2009. The evolution of active galactic nuclei in clusters of galaxies to redshift 1.3. ApJ 701, 66–85. https://doi.org/10.1088/0004-637X/701/1/66, arXiv:0906.1843.

Marziani, P., Deconto-Machado, A., Del Olmo, A., 2022. Isolating an outflow component in single-epoch spectra of quasars. Galaxies 10 (2), 54. https://doi.org/10.3390/galaxies10020054, arXiv:2203.09196.

Marziani, P., D'Onofrio, M., Bettoni, D., et al., 2017. Emission line galaxies and active galactic nuclei in WINGS clusters. A&Ap 599, A83. https://doi.org/10.1051/0004-6361/201628941, arXiv:1608.07924.

Marziani, P., Dultzin, D., Sulentic, J.W., et al., 2018. A main sequence for quasars. Front. Astron. Space Sci. 5, 6. https://doi.org/10.3389/fspas.2018.00006, arXiv:1802.05575.

Marziani, P., Sulentic, J.W., Zwitter, T., et al., 2001. Searching for the physical drivers of the eigenvector 1 correlation space. ApJ 558, 553–560. https://doi.org/10.1086/322286, arXiv:arXiv:astro-ph/0105343.

Mineshige, S., Kawaguchi, T., Takeuchi, M., et al., 2000. Slim-disk model for soft X-ray excess and variability of narrow-line seyfert 1 galaxies. PASJ 52, 499–508, arXiv:arXiv:astro-ph/0003017.

Mishra, H.D., Dai, X., 2020. Lower AGN abundance in galaxy clusters at z < 0.5. AJ 159 (2), 69. https://doi.org/10.3847/1538-3881/ab6225, arXiv:1912.10342.

Mo, W., Gonzalez, A., Brodwin, M., et al., 2020. The massive and distant clusters of WISE survey. VIII. Radio activity in massive galaxy clusters. ApJ 901 (2), 131. https://doi.org/10.3847/1538-4357/abb08d, arXiv:2008.07686.

Mo, W., Gonzalez, A., Stern, D., et al., 2018. The massive and distant clusters of WISE survey. IV. The distribution of active galactic nuclei in galaxy clusters at $z \sim 1$. ApJ 869 (2), 131. https://doi.org/10.3847/1538-4357/aaef83, arXiv:1811.01826.

Moretti, A., Gullieuszik, M., Poggianti, B., et al., 2017. Omega WINGS: spectroscopy in the outskirts of local clusters of galaxies. A&Ap 599, A81. https://doi.org/10.1051/0004-6361/201630030, arXiv:1701.02590.

Osterbrock, D.E., Ferland, G.J., 2006. Astrophysics of Gaseous Nebulae and Active Galactic Nuclei. University Science Books.

Owers, M.S., Couch, W.J., Nulsen, P.E.J., 2009. Substructure in the Cold Front Cluster Abell 3667. ApJ 693 (1), 901–913. https://doi.org/10.1088/0004-637X/693/1/901, arXiv:0811.3031.

Panda, S., Marziani, P., Czerny, B., 2019. The quasar main sequence explained by the combination of eddington ratio, metallicity, and orientation. ApJ 882 (2), 79. https://doi.org/10.3847/1538-4357/ab3292, arXiv:1905.01729.

Peluso, G., Vulcani, B., Poggianti, B.M., et al., 2022. Exploring the AGN-ram pressure stripping connection in local clusters. ApJ 927 (1), 130. https://doi.org/10.3847/1538-4357/ac4225, arXiv:2111.02538.

Pimbblet, K.A., Shabala, S.S., Haines, C.P., et al., 2013. The drivers of AGN activity in galaxy clusters: AGN fraction as a function of mass and environment. MNRAS 429, 1827–1839. https://doi.org/10.1093/mnras/sts470, arXiv:1212.0261.

Poggianti, B.M., Moretti, A., Gullieuszik, M., et al., 2017. GASP.I. Gas stripping phenomena in galaxies with MUSE. ApJ 844 (1), 48. https://doi.org/10.3847/1538-4357/aa78ed, arXiv:1704.05086.

Punsly, B., Marziani, P., Berton, M., et al., 2020. The extreme red excess in blazar ultraviolet broad emission lines. ApJ 903 (1), 44. https://doi.org/10.3847/1538-4357/abb950, arXiv:2009.05082.

Radovich, M., Poggianti, B., Jaffé, Y.L., et al., 2019. GASP - XIX. AGN and their outflows at the centre of jellyfish galaxies. MNRAS 486 (1), 486–503. https://doi.org/10.1093/mnras/stz809, arXiv:1905.08972.

Rakić, N., 2022. Kinematics of the Hα and Hβ broad line region in an SDSS sample of type 1 AGNs. MNRAS. https://doi.org/10.1093/mnras/stac2259, arXiv:2208.04359.

Ramella, M., Biviano, A., Pisani, A., et al., 2007. Substructures in WINGS clusters. A&Ap 470, 39–51. https://doi.org/10.1051/0004-6361:20077245, arXiv:0704.0579.

Richards, G.T., Kruczek, N.E., Gallagher, S.C., et al., 2011. Unification of Luminous Type 1 Quasars through C IV Emission. AJ 141, 167-+. https://doi.org/10.1088/0004-6256/141/5/167, arXiv:1011.2282.

Richards, G.T., Lacy, M., Storrie-Lombardi, L.J., et al., 2006. Spectral energy distributions and multiwavelength selection of type 1 quasars. Ap. J. Suppl. Ser. 166, 470–497. https://doi.org/10.1086/506525, arXiv:arXiv:astro-ph/0601558.

Sdowski, A., Narayan, R., McKinney, J.C., et al., 2014. Numerical simulations of super-critical black hole accretion flows in general relativity. MNRAS 439, 503–520. https://doi.org/10.1093/mnras/stt2479, arXiv:1311.5900.

Shankar, F., Weinberg, D.H., Miralda-Escudé, J., 2013. Accretion-driven evolution of black holes: Eddington ratios, duty cycles and active galaxy fractions. MNRAS 428 (1), 421–446. https://doi.org/10.1093/mnras/sts02610.48550/arXiv.1111.3574, arXiv:1111.3574.

Shen, Y., Ho, L.C., 2014. The diversity of quasars unified by accretion and orientation. Nature 513, 210–213. https://doi.org/10.1038/nature13712, arXiv:1409.2887.

Śniegowska, M., Marziani, P., Czerny, B., et al., 2021. High metal content of highly accreting quasars. ApJ 910 (2), 115. https://doi.org/10.3847/1538-4357/abe1c8, arXiv:2009.14177.

Somboonpanyakul, T., McDonald, M., Noble, A., et al., 2022. The Evolution of AGN Activity in Brightest Cluster Galaxies. AJ 163 (4), 146. https://doi.org/10.3847/1538-3881/ac5030, arXiv:2201.08398.

Souchay, J., Andrei, A.H., Barache, C., et al., 2015. The third release of the Large Quasar Astrometric Catalog (LQAC-3): a compilation of 321 957 objects. A&Ap 583, A75. https://doi.org/10.1051/0004-6361/201526092.

Sulentic, J.W., Marziani, P., Dultzin-Hacyan, D., 2000a. Phenomenology of broad emission lines in active galactic nuclei. ARA&A 38, 521–571. https://doi.org/10.1146/annurev.astro.38.1.521.

Sulentic, J.W., Zwitter, T., Marziani, P., et al., 2000b. Eigenvector 1: An optimal correlation space for active galactic nuclei. ApJL 536, L5–L9. https://doi.org/10.1086/312717, arXiv:arXiv:astro-ph/0005177.

Valentinuzzi, T., Poggianti, B.M., Fasano, G., et al., 2011. The red-sequence of 72 WINGS local galaxy clusters. A&Ap 536, A34. https://doi.org/10.1051/0004-6361/201117522, arXiv:1109.4011.

Veilleux, S., Osterbrock, D.E., 1987. Spectral classification of emission-line galaxies. Ap. J. Suppl. Ser. 63, 295–310. https://doi.org/10.1086/191166.

Vestergaard, M., Peterson, B.M., 2006. Determining central black hole masses in distant active galaxies and quasars. II. Improved optical and UV scaling relationships. ApJ 641, 689–709. https://doi.org/10.1086/500572, arXiv:arXiv:astro-ph/0601303.

von der Linden, A., Wild, V., Kauffmann, G., et al., 2010. Star formation and AGN activity in SDSS cluster galaxies. MNRAS 404, 1231–1246. https://doi.org/10.1111/j.1365-2966.2010.16375.x, arXiv:0909.3522.

Wang, J.-M., Du, P., Valls-Gabaud, D., et al., 2013. Super-eddington accreting massive black holes as long-lived cosmological standards. Phys. Rev. Lett. 110 (8), 081301. https://doi.org/10.1103/PhysRevLett.110.081301, arXiv:1301.4225.

Zamfir, S., Sulentic, J.W., Marziani, P., et al., 2010. Detailed characterization of Hβ emission line profile in low-z SDSS quasars. MNRAS 403, 1759. https://doi.org/10.1111/j.1365-2966.2009.16236.x, arXiv:0912.4306.